

# Derivation of the lattice Boltzmann equation via Method of Characteristics

Huanfeng Ye,<sup>1,\*</sup> Bo Kuang,<sup>1,†</sup> and Yanhua Yang<sup>1,2,‡</sup>

<sup>1</sup>*School of Nuclear Science and Engineering, Shanghai Jiao Tong University, Shanghai 200240, China*

<sup>2</sup>*National Energy Key Laboratory of Nuclear Power Software, Beijing 102209, China*

(Dated: March 20, 2017)

A novel derivation of lattice Boltzmann method (LBM) based on Method of Characteristics is presented in this paper. It is shown that LBM is literally a characteristic-line integral of BGK-Boltzmann equation, and the integrals in velocity space and time space, twisted in traditional LBM theory due to relaxation time solving, are independent. Referring to the classical LBM theory, the derivations of LBM evolution equation, macroscopic equation and discrete equilibrium distribution are demonstrated detailly in this paper. The theory indicates that the integral of time space constructs the LBM evolution equation and relaxation time while the integral of velocity space controls its macroscopic equations. Moreover in the temporal integral of BGK-Boltzmann equation, the approximation of equilibrium distribution along the characteristic line plays a key role, which directly involves the evolution equation and relaxation time of LBM. Thus three approximation models are proposed and numerically evaluated.

## I. INTRODUCTION

In the past few decades, the lattice Boltzmann method (LBM) has been proven as an efficient alternative approach in many computational fluid dynamics (CFD) areas, such as hydrodynamic systems [1, 2], multiphase and multicomponent fluids [3–7], porous media flow [8, 9]. With the rapid development of multi-core super computer and parallel computation, LBM is being more attractive to CFD researchers due to its inherent parallelism. However, the ambiguous theory framework of LBM obstructs researchers to develop customized LBM for their own research areas.

Historically, LBM evolves from the lattice-gas automata (LGA) [10]. In 1992, the prototype of single-relaxation-time LBM was established [11, 12]. At the same time, the multiple-relaxation-time LBM was proposed [13]. In 1997, a rigorous framework of LBM was founded [14], which directly derived LBM from the Bhatnagar-Gross-Krook (BGK) Boltzmann equation [15]. Based on this theory framework, a number of new models have been proposed, creating a golden era of LBM [16–19]. Though LBM has laid a solid theory foundation after decades development, the derivation, twisting the integrals in velocity space and time space due to relaxation time solving [20], confuses the essence that LBM is a Characteristics Method. This misunderstanding has crippled researchers to design LBM models based on their own need.

In this paper, we will show that LBM is a temporal integral of BGK-Boltzmann along the characteristics line, which segregates the integrals in time space and velocity space. Through integrating BGK-Boltzmann equation in time space along the characteristic line, the LBM

evolution equation and relaxation time formula are derived while macroscopic hydrodynamics equations are recovered by integrating in velocity space. As an integral part of the LBM theory, the procedure of discretizing the BGK-Boltzmann equation is also demonstrated by deriving the classical D2Q9 equilibrium distribution model. The analysis shows that standing on the Characteristics Method, the approximation of equilibrium distribution in time space (along the characteristic line) plays a key role on the accuracy of LBM as collision number changes. We propose three approximation models to evaluate it. The numerical results testify the influence of the temporal model. It should be noted that the collision number is the relaxation time  $\Delta t/\lambda$  in BGK-Boltzmann equation. In order to distinguish from the relaxation time  $1/\tau$  in LBM, we rename it as collision number (CN). The kinetic-model equation used in this paper is the BGK-Boltzmann equation with a single relaxation time. Although the single-relaxation-time BGK-Boltzmann equation has its inherent limitation and shortcomings, it is sufficient for us to explore the fundamental of LBM. The derivation in this paper is implemented on two-dimensional space, it's easy to be applied in three-dimensional space.

This paper is organized as follows. In Sec. II, we discuss the derivation of LBM evolution equation from BGK-Boltzmann equation and demonstrate the effect of equilibrium distribution approximation along the characteristic line by proposing three models. In Sec. III, we discuss the recovery of macroscopic hydrodynamic equations corresponding to LBM and formula of collision number. In Sec. IV, we discuss the discretization of LBM and equilibrium distribution. In Sec. V, we demonstrate the effect of the equilibrium distribution temporal model with several simple benchmarks. Section VI concludes the paper.

\* E-mail address: bdqhsjw@sjtu.edu.cn

† E-mail address: bkuang@sjtu.edu.cn

‡ E-mail address: yanhua@sjtu.edu.cn

## II. DERIVATION OF LATTICE BOLTZMANN EVOLUTION EQUATION

The derivation of LBM evolution equation from BGK-Boltzmann has been discussed by a great number of researchers since LBM separated from LGA, but their approaches are quite different [14, 20–22]. We propose that LBM evolution equation is literally the temporal integral of BGK-Boltzmann equation on characteristics line.

BGK-Boltzmann equation is a result of linear approximation on Boltzmann equations collision term [15].

$$\frac{\partial f}{\partial t} + \vec{\xi} \cdot \frac{\partial f}{\partial \vec{r}} = -\frac{1}{\lambda} (f - g) \quad (1)$$

where  $f \equiv f(\vec{r}, \vec{\xi}, t)$  is the particle distribution,  $\vec{\xi}$  is particle's microscopic velocity,  $\lambda$  is the collision time, and  $g$  is the Maxwell-Boltzmann distribution.

$$g \equiv \frac{\rho}{(2\pi RT)^{D/2}} \exp\left(-\frac{(\vec{\xi} - \vec{u})^2}{2RT}\right) \quad (2)$$

where  $R$  is the ideal gas constant,  $D$  is the dimension of the space, and  $\rho$ ,  $\vec{u}$ , and  $T$  are the macroscopic density of mass, velocity and temperature, respectively. The macroscopic variables,  $\rho$ ,  $\vec{u}$ ,  $T$  are the (microscopic velocity) moments of the distribution function,  $f$ :

$$\rho = \int f d\vec{\xi} = \int g d\vec{\xi} \quad (3a)$$

$$\rho \vec{u} = \int \vec{\xi} f d\vec{\xi} = \int \vec{\xi} g d\vec{\xi} \quad (3b)$$

$$\rho RT = \frac{1}{2} \int (\vec{\xi} - \vec{u})^2 f d\vec{\xi} = \frac{1}{2} \int (\vec{\xi} - \vec{u})^2 g d\vec{\xi} \quad (3c)$$

Eq. (1) can be rewritten in the form of an ordinary differential equation:

$$\frac{df}{dt} + \frac{1}{\lambda} f = \frac{1}{\lambda} g \quad (4)$$

where

$$\frac{d}{dt} \equiv \frac{\partial}{\partial t} + \vec{\xi} \cdot \frac{\partial}{\partial \vec{r}}$$

is the time derivative along the characteristic line  $\vec{\xi}$ . Applying the trick in Ref. [14], Eq. (1) can be expressed as

$$\frac{d}{dt} e^{t/\lambda} f = \frac{1}{\lambda} e^{t/\lambda} g \quad (5)$$

Integrating Eq. (5) over a time interval  $\Delta t$ , we can get

$$\begin{aligned} e^{\Delta t/\lambda} f(\vec{r} + \Delta t \vec{\xi}, \vec{\xi}, t + \Delta t) - f(\vec{r}, \vec{\xi}, t) \\ = \frac{1}{\lambda} \int_0^{\Delta t} e^{t'/\lambda} g(\vec{r} + \vec{\xi} t', \vec{\xi}, t + t') dt' \end{aligned} \quad (6)$$

Assuming  $g$  keeps constant during the time interval, steady assumption (SA),

$$g(\vec{r} + \vec{\xi} t', \vec{\xi}, t + t') = g(\vec{r}, \vec{\xi}, t)$$

then Eq. (6) can be expressed as

$$\begin{aligned} e^{\Delta t/\lambda} f(\vec{r} + \Delta t \vec{\xi}, \vec{\xi}, t + \Delta t) - f(\vec{r}, \vec{\xi}, t) \\ = (e^{\Delta t/\lambda} - 1) g(\vec{r}, \vec{\xi}, t) \end{aligned} \quad (7)$$

where  $\Delta t/\lambda$  is collision number, in order to distinguish the relaxation time in LBM. The condition to apply SA is quite strict, the collision number should be small enough, or the equilibrium distribution would seriously depart from the initial state as the collision proceeds, which violates steady assumption (SA). In order to ease the restriction, two approximations of  $g$  temporal function are proposed. The model in Eq. (8a) is called direct correction of deviation (DCD) and in Eq. (8b) evolutionary correction of deviation (ECD). It should be noted that these two approximations are priori, which are derived from classical LBM evolution equations, and due to the integral, the forms are not monotonous.

$$\begin{aligned} g(\vec{r} + \vec{\xi} t', \vec{\xi}, t + t') = g(\vec{r}, \vec{\xi}, t) + f(\vec{r} + \vec{\xi} t', \vec{\xi}, t + t') \\ - f(\vec{r}, \vec{\xi}, t) \end{aligned} \quad (8a)$$

$$\begin{aligned} g(\vec{r} + \vec{\xi} t', \vec{\xi}, t + t') = g(\vec{r}, \vec{\xi}, t) + f(\vec{r} + \vec{\xi} t', \vec{\xi}, t + t') \\ - \tilde{f}(\vec{r} + \vec{\xi} t', \vec{\xi}, t + t') \end{aligned} \quad (8b)$$

with

$$\begin{aligned} \tilde{f}(\vec{r} + \vec{\xi} t', \vec{\xi}, t + t') = f(\vec{r}, \vec{\xi}, t) \\ + \frac{t'}{\Delta t} (f(\vec{r} + \vec{\xi} \Delta t, \vec{\xi}, t + \Delta t) - f(\vec{r}, \vec{\xi}, t)) \end{aligned}$$

The temporal integrals of BGK-Boltzmann equation with approximations in Eq. (8) are

$$\begin{aligned} f(\vec{r} + \Delta t \vec{\xi}, \vec{\xi}, t + \Delta t) - f(\vec{r}, \vec{\xi}, t) \\ = -\frac{\Delta t}{\lambda} (f(\vec{r}, \vec{\xi}, t) - g(\vec{r}, \vec{\xi}, t)) \end{aligned} \quad (9a)$$

$$\begin{aligned} f(\vec{r} + \Delta t \vec{\xi}, \vec{\xi}, t + \Delta t) - f(\vec{r}, \vec{\xi}, t) \\ = -\frac{\Delta t}{\lambda} (\tilde{f} - g(\vec{r}, \vec{\xi}, t)) \end{aligned} \quad (9b)$$

with

$$\tilde{f} = \frac{1}{2} (f(\vec{r} + \Delta t \vec{\xi}, \vec{\xi}, t + \Delta t) + f(\vec{r}, \vec{\xi}, t))$$

Introducing the LBM evolution equation form with relaxation time  $1/\tau$ , the temporal integrals of BGK-Boltzmann equation with SA, DCD, and ECD can read

as

$$\begin{aligned} & f(\vec{r} + \Delta t \vec{\xi}, \vec{\xi}, t + \Delta t) - f(\vec{r}, \vec{\xi}, t) \\ &= -\frac{1}{\tau} \left( f(\vec{r}, \vec{\xi}, t) - g(\vec{r}, \vec{\xi}, t) \right) \end{aligned} \quad (10)$$

with

$$\frac{1}{\tau} = \begin{cases} 1 - e^{-\Delta t/\lambda}, & \text{SA} \\ \frac{\Delta t}{\lambda}, & \text{DCD} \\ 1/(0.5 + \frac{\lambda}{\Delta t}), & \text{ECD} \end{cases} \quad (11)$$

### III. DERIVATION OF MACROSCOPIC EQUATIONS

The macroscopic equations are used to solve the relaxation time and analyse the model of discrete equilibrium distribution. As demonstrated in the Sec. II, LBM is the integral of BGK-Boltzmann equation with temporal approximation on equilibrium distribution. It's irrelevant to the integral in velocity space which is used to recover the macroscopic hydrodynamic equations. To be specific, BGK-Boltzmann equation is the real control equation for the physical process at certain moment while LBM evolution equation is the integration of the process on timestep  $\Delta t$  along characteristic line  $\vec{\xi}$ . Meanwhile the macroscopic equations are the control equations of macro properties at certain moment. Therefore, we employ original BGK-Boltzmann equation to recover hydrodynamic equations instead of LBM evolution equation in classical LBM. The recovery is achieved by implementing traditional Chapman-Enskog (CE) expansion. To avoid struggling in the diverse equilibrium distribution models, we take Maxwell-Boltzmann distribution as the equilibrium distribution. It's straightforward to extend the procedure in specific discrete equilibrium distribution models.

The CE expansion is a multiple scale technology, proposed to solve the Boltzmann equation at first [23]. When LBM established its theory on BGK-Boltzmann equation, this approach has become the analyse methodology of LBM inherently. The key concept of CE expansion is formulating the flow phenomena with different time scales. Firstly, we decompose the partial differential of time and space into different scales

$$\frac{\partial}{\partial t} = \varepsilon \frac{\partial}{\partial t_1} + \varepsilon^2 \frac{\partial}{\partial t_2} + \dots \quad (12a)$$

$$\frac{\partial}{\partial \vec{r}} = \varepsilon \frac{\partial}{\partial \vec{r}_1} \quad (12b)$$

where  $\varepsilon$  is a small parameter to identify the scales,  $t_i$  and  $\vec{r}_i$  is the relative time and space scales respectively. Specifically,  $t_1$  and  $t_2$  represents the time scale of convection and diffusion respectively [24]. Similarly, we expand the particle distribution  $f$  with parameter  $\varepsilon$

$$f = g + \sum_{n=1}^{\infty} \varepsilon^n f^{(n)} \quad (13)$$

where  $g$  is the Maxwell-Boltzmann distribution. It should be noted, this expansion implies that the deviation between particle distribution  $f$  and equilibrium distribution  $g$  is limited. Combining with the macroscopic variables formula in Eq. (3), the integrals of the expansion for macroscopic variables lead to

$$\int \sum_{n=1}^{\infty} \varepsilon^n f^{(n)} d\vec{\xi} = 0 \quad (14a)$$

$$\int \sum_{n=1}^{\infty} \varepsilon^n f^{(n)} \vec{\xi} d\vec{\xi} = \vec{0} \quad (14b)$$

$$\int \sum_{n=1}^{\infty} \varepsilon^n f^{(n)} (\vec{\xi} - \vec{u})^2 d\vec{\xi} = 0 \quad (14c)$$

In order to solve the BGK-equation, CE expansion employs an extra assumption, that the first three velocity moment integrals of the decomposed distribution equals zero on each order of  $\varepsilon$ . For sake of simplicity but without losing generality, we use a linear combination of first three moments  $\phi(\vec{\xi})$  to describe the assumption,

$$\int f^{(n)} \phi(\vec{\xi}) d\vec{\xi} = 0 \quad (15)$$

where

$$\phi(\vec{\xi}) = A + \vec{B} \cdot \vec{\xi} + C\xi^2$$

where  $A$  and  $C$  are arbitrary constants,  $\vec{B}$  is arbitrary constant vector.

Now, substituting the expansions in Eq. (12) and Eq. (13) into BGK-Boltzmann equation in Eq. (1) and collecting all terms with first two orders of  $\varepsilon$  leads to:

$$\frac{\partial g}{\partial t_1} + \vec{\xi} \cdot \frac{\partial g}{\partial \vec{r}_1} = -\frac{1}{\lambda} f^{(1)} \quad (16a)$$

$$\frac{\partial g}{\partial t_2} + \frac{\partial f^{(1)}}{\partial t_1} + \vec{\xi} \cdot \frac{\partial f^{(1)}}{\partial \vec{r}_1} = -\frac{1}{\lambda} f^{(2)} \quad (16b)$$

Integrating Eq. (16) on the first two velocity moments with the assumption in Eq. (15), we can get

$$\frac{\partial \rho}{\partial t_1} + \frac{\partial \rho \vec{u}}{\partial \vec{r}_1} = 0 \quad (17a)$$

$$\frac{\partial \rho \vec{u}}{\partial t_1} + \frac{\partial \rho \vec{u} \vec{u}}{\partial \vec{r}_1} + \frac{\partial \rho RT}{\partial \vec{r}_1} = 0 \quad (17b)$$

$$\frac{\partial \rho}{\partial t_2} = 0 \quad (18a)$$

$$\frac{\partial \rho \vec{u}}{\partial t_2} + \frac{\partial}{\partial \vec{r}} \cdot \left( -\rho RT \lambda \left( [\nabla \vec{u}] + [\nabla \vec{u}]^T \right) \right) = 0 \quad (18b)$$

Incorporating the formulas in Eq. (17) and Eq. (18) based on their order of velocity moment respectively, the macroscopic hydrodynamic equations are recovered for BGK-Boltzmann equation with Maxwell-Boltzmann distribution.

$$\frac{\partial \rho}{\partial t} + \frac{\partial \rho \vec{u}}{\partial \vec{r}} = 0 \quad (19a)$$

$$\begin{aligned} \frac{\partial \rho}{\partial t} + \frac{\partial \rho \vec{u}}{\partial \vec{r}} &= -\frac{\partial p}{\partial \vec{r}} \\ &+ \frac{\partial}{\partial \vec{r}} \cdot \left( \nu \rho \left( [\nabla \vec{u}] + [\nabla \vec{u}]^T \right) \right) \end{aligned} \quad (19b)$$

where  $p = \rho RT$  is the pressure,  $\nu = RT\lambda$  is the kinematic viscosity. Then the collision time  $\lambda$  can be solved as

$$\lambda = \frac{\nu}{RT} \quad (20)$$

and relaxation time  $1/\tau$  in LBM equals

$$\frac{1}{\tau} = \begin{cases} 1 - e^{RT\Delta t/\nu}, & \text{SA} \\ \frac{RT\Delta t}{\nu}, & \text{DCD} \\ 1/\left(0.5 + \frac{\nu}{RT\Delta t}\right), & \text{ECD} \end{cases} \quad (21)$$

#### IV. DISCRETIZATION OF THE LATTICE BOLTZMANN EQUATION AND ITS EQUILIBRIUM DISTRIBUTION FUNCTION

In the former two sections, we have discussed the derivation of LBM evolution equation and relaxation time  $1/\tau$ , the solution of collision time  $\lambda$ . The discussion is based on continuous BGK-Boltzmann equation. Though it wouldn't interfere the understanding of LBM theory, the continuous BGK-Boltzmann equation need discretizing in velocity space before practical application. The discretion includes discretizing the velocity space of particle distribution and constructing the equilibrium distribution based on the discrete-velocity model. Technically speaking, the discrete equilibrium distribution model determines the final recovery form of hydrodynamic equations, such as compressible or incompressible equations, conduct equation and so on, but it is out of this paper's discussion. Here we prefer to offer a solution for researchers to develop their own model and complete our theory. This approach has been discussed detailly in Ref. [14]. For sake of simplicity but without losing generality, we employ 2-dimensional Maxwell-Boltzmann distribution to construct the classical D2Q9 model. The derivation can be easily extended in 3 dimension and constructing new models.

The key to construct a discrete equilibrium distribution is to keep the relative velocity moment integrals consistent with target distribution. For an instance, wthe following velocity moment integrals in Eq. (22) have been used in Sec. III to recover the hydrodynamic equations. So the discrete model should be evaluated on moments  $1, \vec{\xi}, \dots, \vec{\xi}^3$ .

$$\rho : 1, \xi_\alpha, \xi_\alpha \xi_\beta \quad (22a)$$

$$\rho \vec{u} : \xi_\alpha, \xi_\alpha \xi_\beta, \xi_\alpha \xi_\beta \xi_\gamma \quad (22b)$$

where  $\xi_\alpha$  is the component of  $\vec{\xi}$  in Cartesian coordinates.

Firstly, exponent part in the Maxwell-Boltzmann distribution is decomposed: one for the weight function, the other for the distribution with respect to macro velocity.

$$g \equiv \frac{\rho}{(2\pi RT)^{D/2}} \exp\left(-\frac{\xi^2}{2RT}\right) \exp\left(-\frac{u^2 - 2\vec{u} \cdot \vec{\xi}}{2RT}\right) \quad (23)$$

For the convenience of calculating weights, the truncated small velocity expansion (or low-Mach-number approximation) is employed. Consulting Ref. [14], the terms above 2nd macro-velocity order are neglected.

$$\begin{aligned} g' &= \frac{\rho}{(2\pi RT)^{D/2}} \exp\left(-\frac{\xi^2}{2RT}\right) \\ &\times \left( 1 + \frac{\vec{\xi} \cdot \vec{u}}{RT} + \frac{(\vec{\xi} \cdot \vec{u})^2}{2(RT)^2} - \frac{u^2}{2RT} \right) + O(u^3) \end{aligned} \quad (24)$$

It's important to note that the order of low-Mach-number approximation decides the velocity moment integrals' accuracy of  $g'$ , which means the order of velocity moment integral that  $g'$  can restore. Taking Eq. (24) for example, the 2nd order truncation could only restore the velocity moment integral up to 2nd order. The 3rd order moment integral of the truncated Maxwell-Boltzmann distribution in Eq. (26) would deviate from the original in Eq. (25).

$$\begin{aligned} \int g \xi_\alpha \xi_\beta \xi_\gamma &= \rho u_\alpha u_\beta u_\gamma + u_\gamma \rho RT \delta_{\alpha\beta} \\ &+ u_\beta \rho RT \delta_{\alpha\gamma} + u_\alpha \rho RT \delta_{\beta\gamma} \end{aligned} \quad (25)$$

$$\int g' \xi_\alpha \xi_\beta \xi_\gamma = u_\gamma \rho RT \delta_{\alpha\beta} + u_\beta \rho RT \delta_{\alpha\gamma} + u_\alpha \rho RT \delta_{\beta\gamma} \quad (26)$$

To keep equivalent on 3rd velocity moment integral,  $g'$  need to maintain macro-velocity terms up to 3rd order. Here are 3rd order approximation (seeing Eq. (27)) and its 3rd velocity moment integral (seeing Eq. (28)).

$$g' = \frac{\rho}{(2\pi RT)^{D/2}} \exp\left(-\frac{\xi^2}{2RT}\right) \left(1 + \frac{2\vec{\xi} \cdot \vec{u} - u^2}{2RT} + \frac{1}{2} \left(\frac{\vec{\xi} \cdot \vec{u}}{RT}\right)^2 + \frac{1}{2} \left(\frac{-\vec{\xi} \cdot \vec{u}^3}{(RT)^2}\right) + \frac{1}{6} \left(\frac{\vec{\xi} \cdot \vec{u}}{RT}\right)^3\right) \quad (27)$$

$$\int g' \xi_\alpha \xi_\beta \xi_\gamma = \rho u_\alpha u_\beta u_\gamma + u_\gamma \rho RT \delta_{\alpha\beta} + u_\beta \rho RT \delta_{\alpha\gamma} + u_\alpha \rho RT \delta_{\beta\gamma} \quad (28)$$

Unfortunately, the implementation of 3rd order approximation needs extremely complicated velocity discretization. In this paper, the 2nd order approximation is still to be stick with.

After low-Mach-number approximation, the target continuous equilibrium distribution has been  $g'$  instead of original Maxwell-Boltzmann distribution  $g$ . Right now,  $g'$  in Eq. (24) bears a strong resemblance to the classical D2Q9 equilibrium distribution, all remains to be accomplished is calculating the weight of discrete velocity. As

we discussed before, the discrete equilibrium model  $f^{eq}$  should keep the velocity moment integrals required in Eq. (22) consistent with  $g'$ .

$$\sum \psi(\vec{\xi}_\alpha) f_\alpha^{eq} = \int \psi(\vec{\xi}) g' d\vec{\xi} \quad (29)$$

where  $\psi(\vec{\xi})$  is a polynomial of  $\vec{\xi}$  up to order 3. For the sake of simplicity but without losing generality, assuming

$$\psi(\vec{\xi}) = \psi_{m,n}(\vec{\xi}) = \xi_x^m \xi_y^n, m+n \leq 3 \quad (30)$$

then the velocity moment integrals of  $g'$  can read as

$$\int \psi(\vec{\xi}) g' d\vec{\xi} = \frac{\rho}{\pi} \left( \left(1 - \frac{u^2}{2RT}\right) (\sqrt{2RT})^{m+n} I_m I_n + \frac{1}{RT} (\sqrt{2RT})^{m+n+1} (u_x I_{m+1} I_n + u_y I_m I_{n+1}) + (\sqrt{2RT})^{m+n+2} \frac{(I_{m+2} I_n u_x^2 + 2I_{m+1} I_{n+1} u_x u_y + I_m I_{n+2} u_y^2)}{2(RT)^2} \right) \quad (31)$$

with

$$I_m = \int e^{-x^2} x^m dx, x = \xi/\sqrt{2RT} \quad (32)$$

which can be calculated numerically with Gaussian-type quadrature. Our object is using proper discretization of velocity space to evaluate the integral  $I_m$  with  $m$  up to 5. Naturally, the third-order Hermite formula [14] is the optimal choice for the purpose of deriving the D2Q9 model.

$$I_m = \int \exp^{-x^2} x^m dx = \sum \omega_i x_i^m \quad (33)$$

The integrals need to be evaluated are,  $I_0, I_2, I_4$ . Other integrals with odd order of  $x$  equals 0 due to the symmetry of Eq. (33) which can be easily solved by using symmetrical abscissas of the quadrature. Setting the abscissas of quadrature as  $x_0 = 0, x_1 = -\zeta, x_2 = \zeta$ , we have

the following three equations:

$$I_0 = \omega_0 + \omega_1 + \omega_2 = \sqrt{\pi} \quad (34a)$$

$$I_2 = \omega_1 \zeta^2 + \omega_2 \zeta^2 = \sqrt{\pi}/2 \quad (34b)$$

$$I_4 = \omega_1 \zeta^4 + \omega_2 \zeta^4 = 3\sqrt{\pi}/4 \quad (34c)$$

with symmetrical weights

$$\omega_1 = \omega_2 \quad (35)$$

The three abscissas of the quadrature are

$$x_0 = 0, x_1 = -\sqrt{3/2}, x_2 = \sqrt{3/2} \quad (36)$$

and the corresponding weight coefficients are

$$\omega_0 = 2\sqrt{\pi}/3, \omega_1 = \sqrt{\pi}/6, \omega_2 = \sqrt{\pi}/6 \quad (37)$$

Then the evaluation Eq. (29) can read as

$$\sum \psi(\vec{\xi}_\alpha) f_\alpha^{eq} = \int \psi(\vec{\xi}) g' d\vec{\xi} = \frac{\rho}{\pi} \sum_{i,j=0}^2 \omega_i \omega_j \psi(\vec{\xi}_{i,j}) \left(1 + \frac{\vec{\xi}_{i,j} \cdot \vec{u}}{RT} + \frac{(\vec{\xi}_{i,j} \cdot \vec{u})^2}{2(RT)^2} - \frac{u^2}{2RT}\right) \quad (38)$$

where  $\vec{\xi}_\alpha = \vec{\xi}_{i,j} = \sqrt{2RT} (x_i, x_j)$ . It's straightforward to

identify the discrete equilibrium distribution with

$$f_i^{eq} = \frac{1}{\pi} \omega_i \omega_j \left(1 + \frac{\vec{\xi}_{i,j} \cdot \vec{u}}{RT} + \frac{(\vec{\xi}_{i,j} \cdot \vec{u})^2}{2(RT)^2} - \frac{u^2}{2RT}\right) \quad (39)$$

Combining with the notations of discrete velocity and corresponding weights, employing the relation  $RT = c_s^2 = c^2/3$ , a complete D2Q9 model is constructed

$$f_\alpha^{eq} = w_\alpha \rho \left( 1 + \frac{\vec{\xi}_\alpha \cdot \vec{u}}{c_s^2} + \frac{(\vec{\xi}_\alpha \cdot \vec{u})^2}{2c_s^4} - \frac{u^2}{2c_s^2} \right) \quad (40)$$

with discrete velocity,

$$\vec{\xi}_\alpha = \begin{cases} (0, 0), & \alpha = 0 \\ (\cos \theta_\alpha, \sin \theta_\alpha) c, & \alpha = 1, 2, 3, 4 \\ \sqrt{2} (\cos \theta_\alpha, \sin \theta_\alpha) c, & \alpha = 5, 6, 7, 8 \end{cases} \quad (41)$$

where

$$\theta_\alpha = \begin{cases} (\alpha - 1) \pi / 2, & \alpha = 1, 2, 3, 4 \\ (\alpha - 5) \pi / 2 + \pi / 4, & \alpha = 5, 6, 7, 8 \end{cases}$$

and weights

$$w_\alpha = \frac{\omega_i \omega_j}{\pi} = \begin{cases} 4/9, & \alpha = 0 \\ 1/9, & \alpha = 1, 2, 3, 4 \\ 1/36, & \alpha = 5, 6, 7, 8 \end{cases} \quad (42)$$

where  $\rho = \sum f_\alpha$ ,  $\vec{u} = \sum f_\alpha \vec{\xi}_\alpha / \rho$ .

## V. NUMERICAL RESULTS

All the ingredients constructing a LBM with D2Q9 model have been derived until now: evolution equation, relaxation time and discrete equilibrium distribution. The derivation indicates that the approximation of  $g(\vec{r} + \vec{\xi} t', \vec{\xi}, t + t')$  plays a key role on the accuracy of a single-relax-time LBM. So in this section, we would like to demonstrate this influence quantitatively. In the former derivations, we have gotten the following LBM equations corresponding to D2Q9 model

$$f_\alpha^{n+1} - f_\alpha^n = -\frac{1}{\tau} (f_\alpha^n - f_\alpha^{n,eq}) \quad (43)$$

with relaxation time

$$\frac{1}{\tau} = \begin{cases} 1 - e^{-\Delta t / \lambda} = 1 - e^{c_s^2 \Delta t / \nu}, & \text{SA} \\ \frac{c_s^2 \Delta t}{\nu}, & \text{DCD} \\ 1 / \left( 0.5 + \frac{\nu}{c_s^2 \Delta t} \right), & \text{ECD} \end{cases} \quad (44)$$

where  $f_\alpha^{n+1}$  is the particle distribution corresponding to  $t = (n+1) \Delta t$ ,  $\vec{r} = \vec{r}_o + \vec{\xi}_\alpha \Delta t$ ,  $\vec{\xi} = \vec{\xi}_\alpha$ ,  $f_\alpha^n$  is the particle distribution corresponding to  $t = n \Delta t$ ,  $\vec{r} = \vec{r}_o$ ,  $\vec{\xi} = \vec{\xi}_\alpha$ ,  $f_\alpha^{n,eq}$  is the equilibrium distribution corresponding to  $t = n \Delta t$ ,  $\vec{r} = \vec{r}_o$ ,  $\vec{\xi} = \vec{\xi}_\alpha$  (seeing Eq. (40)), and  $c_s^2 \Delta t / \nu$  is the collision number. As Eq. (44) shows, ECD relaxation time is the same with classical single relaxation time. In fact, ECD approximation is a reverse engineering for classical single-relax-time LBM, it's priori. The demonstration would be arranged as followings. Firstly the performance of relaxation times will be analysed, with respect

to collision time, based on SA, DCD and ECD. Then two benchmarks, unsteady Couette flow and lid-driven cavity flow, will be calculated employing D2Q9 model with SA and ECD. The results of SA and ECD will be compared to analyse their accuracy under different collision numbers and validate the effect of temporal approximation models. In the calculation of benchmarks, the DCD approximation will be abandoned due to its instability.

### A. Relax time

As Eq. (44) shows, for the same calculation, which means having the same collision number  $\Delta t / \lambda$ , the proposed approximation models, SA, DCD and ECD, only differ in relaxation time  $1/\tau$ . Fig. 1 illustrates the relaxation time profiles of SA, DCD and ECD with respect to collision number. For  $\Delta t / \lambda \rightarrow 0$ , SA, DCD and ECD approaches each other. As the collision number increases, all three relaxation times increase with different rate, which leads to  $1/\tau_{DCD} > 1/\tau_{ECD} > 1/\tau_{SA}$ . When the collision number goes into infinite, SA and ECD relaxation time would converge to 1 and 2 respectively, while DCD increase unlimitedly, which causes the instability of DCD.

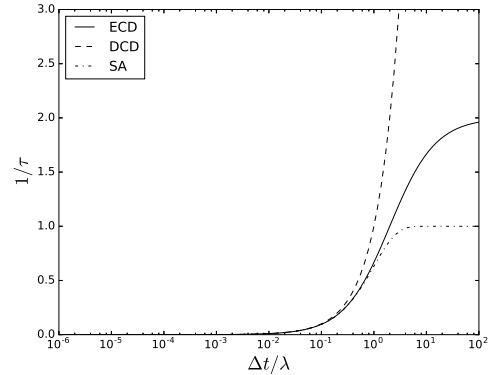


FIG. 1: relaxation time vs collision number. the solid, dashed and dashdot line is ECD, DCD and SA result, respectively. Note that the result of DCD is truncated by the limitation of relaxation time.

### B. Unsteady Couette flow

Unsteady Couette flow, also as known as transient plane Couette flow, is a common numerical benchmark. It evolves in a straight channel, which infinitely extends in the x direction. The walls of the channel are parallel to the x axis and defined by the equations  $y = 0$  for the lower wall and  $y = L$  for the upper wall. The flow is stationary at the beginning and driven by the upper wall with a constant velocity after that. Its equation can be

described as

$$\frac{\partial u(y, t)}{\partial t} = \nu \frac{\partial^2 u(y, t)}{\partial y^2} \quad (45)$$

with the following initial and boundary conditions in the range of  $0 \leq y \leq L$

$$u(0, t) = 0, \quad u(L, t) = U, \quad u(0, t) = 0 \quad (46)$$

where  $\nu$  is kinematic viscosity,  $U$  is the upper wall's driven velocity,  $L$  is the width of channel. Unsteady Couette flow can be solved analytically:

$$u(y, t) = U \frac{y}{L} - \frac{2U}{\pi} \sum_{k=1}^{\infty} \frac{1}{k} \sin\left(k\pi \left(1 - \frac{y}{L}\right)\right) e^{-\frac{k^2 \pi^2}{L^2} \nu t} \quad (47)$$

The periodic boundary is implemented on x direction to simulate the infinite extension. For the upper and lower wall, the regularized boundary [19] is applied. Actually, in unsteady Couette flow, Zou-He boundary [25] and Inamuro boundary [26] would share the same macro result with regularized boundary, though the distributions may differ. 5 cases are designed to discuss the SA and ECD models, listed in Table I. Each case has two states: low collision number(LCN) and high collision number(HCN). Fig. 2 shows the SA and ECD velocity profiles of unsteady Couette flow at  $t = 1.00E - 3$  s. Fig. 3 illustrates the error evolution on time. The error formula is defined as

$$Error = \frac{\sum (u - u_{ana})}{\sum u_{ana}} \quad (48)$$

where  $u$  is the computing velocity profile,  $u_{ana}$  is the analytical velocity profile.

TABLE I: Configurations of unsteady Couette flow demonstrating cases. For all cases, the channel width equals  $L = 0.1$  m, and the driven velocity of upper wall is  $U = 1.0$  m/s.

Case name	CN <sup>a</sup> type	Grid number <sup>b</sup>	Timestep	Kinematic viscosity	Collision number
case1	LCN	201	2.50E-4	1.00E-3	3.33E-1
	HCN		2.50E-6		3.33E+1
case2	LCN	101	1.00E-4	1.00E-2	3.33E-1
	HCN		1.00E-6		3.33E+1
case3	LCN	101	2.00E-5	5.00E-2	3.33E-1
	HCN		2.00E-7		3.33E+1
case4	LCN	101	1.00E-5	1.00E-1	3.33E-1
	HCN		1.00E-7		3.33E+1
case5	LCN	101	1.00E-6	1.00E+0	3.33E-1
	HCN		1.00E-8		3.33E+1

<sup>a</sup> CN stands for collision number

<sup>b</sup> Grid number is the mesh number on cavity side length  $L$

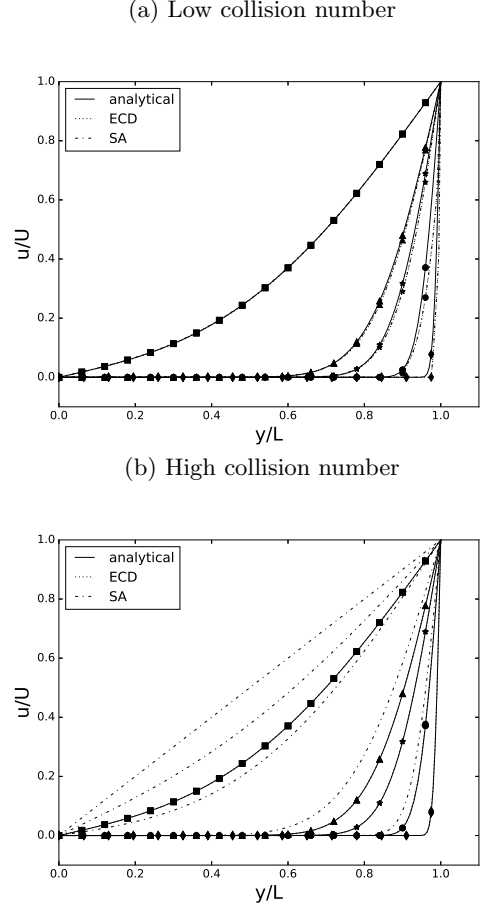


FIG. 2: The velocity profiles of unsteady Couette flow at  $t = 1.00E - 3$  s: (a) low collision number; (b) high collision number. The symbols  $\blacksquare$ ,  $\blacktriangle$ ,  $\star$ ,  $\bullet$ ,  $\blacklozenge$  are results of case1, case2, case3, case4, case5, respectively. Under low collision number in Fig. 2a, models agree well with each other, and share a similar profile with analytical solution. Under high collision number in Fig. 2b, ECD keeps consistent with analytical solution while SA fails. Note the detail descriptions of cases are listed in Table I.

For the sake of space saving, only the error evolutions of case1, case3 and case5 are plotted. As the velocity profiles in Fig. 2 shows, at low collision number, SA and ECD have almost the same velocity profile due to the similar relaxation time. Meanwhile at high collision number, as the SA assumption is invalid, SA fails to capture the velocity profiles while ECD still keeps the similar profiles. The error evolution in Fig. 3 confirms the same conclusion. The results of unsteady Couette flow indicate that SA is a proper model for low collision number, and the assumption would fail at high collision number. Meanwhile the ECD model functions reliably under both low and high collision number. The differential performance of SA and ECD validates the effect of equilibrium distribution's temporal model on accuracy of LBM.

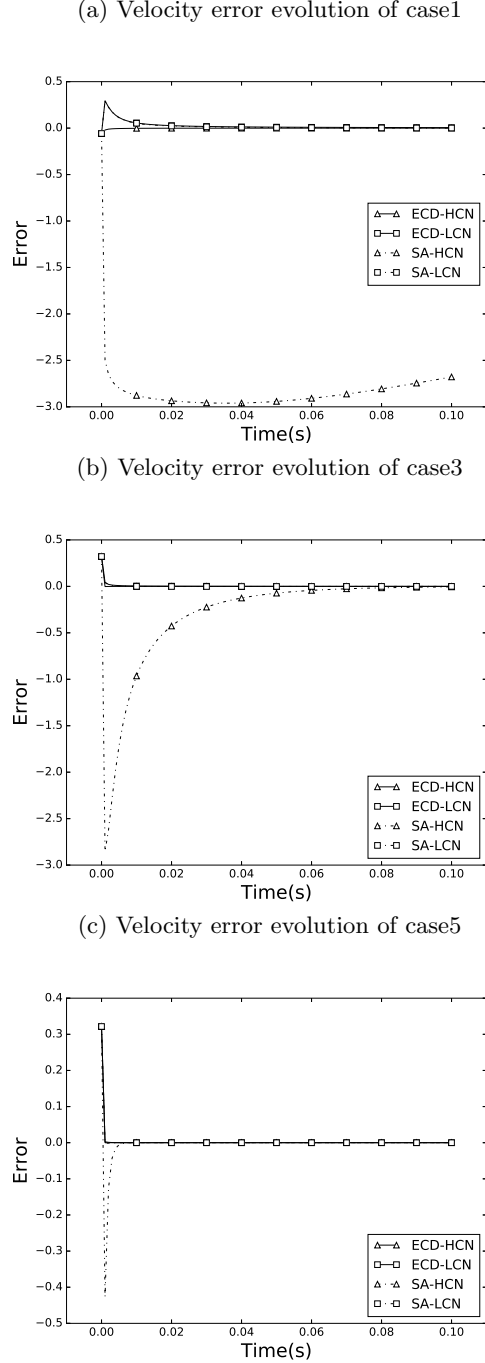


FIG. 3: Velocity error evolution of unsteady Couette flow: (a) case1 result; (b) case3 result; (c) case5 result. ECD-HCN, ECD-LCN, SA-HCN, SA-LCN stand for results of ECD model with low collision number(LCN), ECD model with high collision number(HCN), SA model with low collision number(LCN), SA model with high collision number(HCN), respectively.

### C. Lid-driven cavity flow

Lid-driven cavity flow is a classical constant-property benchmark for fluid computation, for its simple geometry and complicated flow behaviors, especially the corner flow phenomena. Lid-driven cavity flow is a 2-D case characterized by Renold (Re) number, which develops in a square cavity with the side length  $L$ . The fluid would keep stationary at the beginning and be driven by the top lid with constant velocity after that. Except the top lid, all other walls keep rest. This case has no analytic solution. As a convention, the results in Ref. [27] are taken as a calibration on velocity profiles. As the definition of collision number shows, with small kinematic viscosity, the collision number is inherently large. It's very difficult to simulate a high Re-number cavity flow under low collision number without mesh explosion. Fortunately, our mission is to evaluate the approximation models by collision number instead of Re number. A small Re-number case with different collision numbers can fulfill the task. Hence the case with smallest Re number in Ref. [27],  $Re = 100$ , is calculated for analysis. It's configured as Table II. The cavity sides and corners employ the regularized boundary [19]. Fig. 4 illustrates the velocity profiles along the vertical and horizontal lines through cavity center. The models keep consistent with their performance in Sec. VB, under low collision number (LCN), SA and ECD share a close profile; under high collision number (HCN), ECD sticks with the low-collision-number profile while SA fails. To give a full picture of the calculations, the vorticity contours are plotted in Fig. 5, which can be quantified by post-processing software compared to streamline. The values of vorticity along contours are 0,  $\pm 0.5$ ,  $\pm 1.0$ ,  $\pm 2.0$ ,  $\pm 3.0$ , 4.0, 5.0. As Fig. 5 depicts, under LCN, SA (seeing Fig. 5b) and ECD (seeing Fig. 5a) have the same vorticity contour; under HCN, though the contour of ECD in Fig. 5c is a bit dispersed, the shape agrees well with LCN result while SA (seeing Fig. 5d) is quite different. As a conclusion, the results of Lid-driven cavity testify the effect of equilibrium distribution's temporal model on accuracy of LBM.

TABLE II: Configurations of lid-driven cavity flow. The cavity side length equals 1.0m, the driven-lid velocity is 1.0m/s

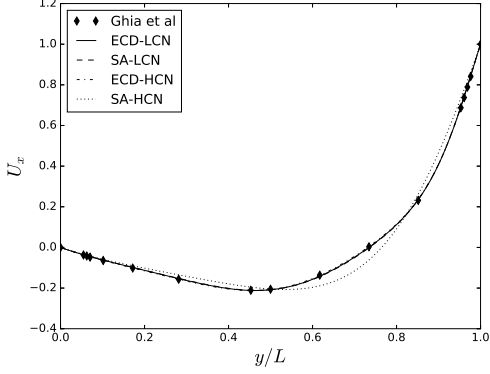
CN <sup>a</sup> type	Grid number <sup>b</sup>	Timestep	Kinematic viscosity	Collision number
LCN	257	1.00E-3	1.00E-2	5.09E-1
HCN		1.00E-6		5.09E+2

<sup>a</sup> CN stands for collision number

<sup>b</sup> Grid number is the mesh number on cavity side length  $L$



(a) Velocity profiles of  $U_x$  along the vertical line through cavity center



(b) Velocity profiles of  $U_y$  along the horizontal line through cavity center

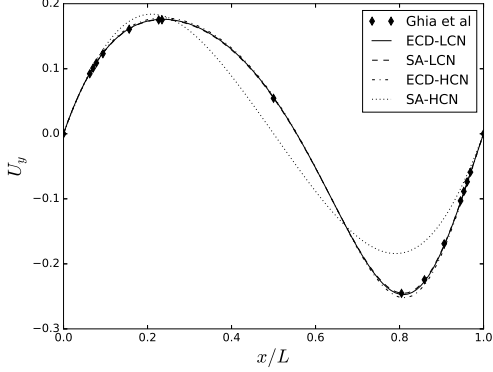


FIG. 4: Velocity profiles along the lines through cavity center. The line with label *Ghia et al* is the calibration from Ref. [27]

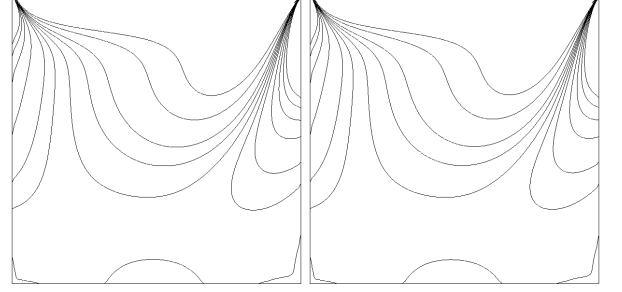
## VI. DISCUSSION AND CONCLUSION

In this paper, we have presented a derivation from BGK-Boltzmann equation to LBM via Method of Characteristics. The derivation shows LBM is a literally characteristic-line integral of BGK-Boltzmann equation. The evolution equation and relaxation time of LBM depend on the temporal approximation of equilibrium distribution along the characteristic line while the macroscopic equations corresponding to LBM are controlled by original BGK-Boltzmann equation. It departs the integral in time space from integral in velocity space, which are twisted in classical LBM theory due to relaxation time solving. Besides, the discrete LBM and equilibrium distribution are discussed in detail. As the derivation shows, the temporal approximation of equilibrium distribution plays a key role on the accuracy and stability

of LBM. Thus we propose three approximation models, SA, ECD and DCD, and evaluate them numerically. The results confirm the influences of the temporal models.

(a) ECD under LCN

(b) SA under LCN



(c) ECD under HCN

(d) SA under HCN

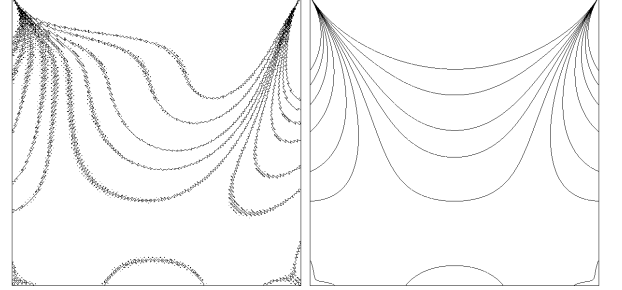


FIG. 5: Vorticity contours of the cavity flow. The values of vorticity along contours are 0,  $\pm 0.5$ ,  $\pm 1.0$ ,  $\pm 2.0$ ,  $\pm 3.0$ , 4.0, 5.0.

The theory in this paper offers a clear physical process of LBM by segregating the integrals of time space and velocity space. LBM is a temporal integral along the characteristic line. This temporal integral generates the evolution equation and relaxation time based on the approximation of equilibrium distribution. Meanwhile the macroscopic equations is determined by the BGK-Boltzmann equation and equilibrium distribution. With these two concepts, we can look forward to improving the accuracy of LBM under the same macroscopic equations by developing temporal approximation of equilibrium distribution and designing special macroscopic equations, conduct equation, wave equation and so on, with customized equilibrium distribution or even customized "Boltzmann" equation.

## ACKNOWLEDGMENTS

The author would like to express his gratitude to Dr. Zecheng Gan for helpful discussion, and to Dr. Mathias J. Krause for generous support on OpenLB software. The author is also grateful to the OpenLB team for their open source sharing ([www.openlb.net](http://www.openlb.net)).

- 
- [1] H. Liu, C. Zou, B. Shi, Z. Tian, L. Zhang, and C. Zheng, *Int. J. Heat Mass Tran.* **49**, 4672 (2006).
  - [2] S. Baochang and G. Zhaoli, *Int. J. Mod. Phys. B* **17**, 173 (2003).
  - [3] A. J. C. Ladd and R. Verberg, *J. Stat. Phys.* **104**, 1191 (2001).
  - [4] M. Sheikholeslami, M. Gorji-Bandpy, and D. D. Ganji, *Powder Technol.* **254**, 82 (2014).
  - [5] X. Liu and P. Cheng, *Int. J. Heat Mass Tran.* **64**, 1041 (2013).
  - [6] E. Semma, M. E. Ganaoui, R. Bennacer, and A. A. Mohamad, *Int. J. Therm. Sci.* **47**, 201 (2008).
  - [7] L. Mountrakis, E. Lorenz, O. Malaspinas, S. Alowayyed, B. Chopard, and A. G. Hoekstra, *J. Comput. Sci.-Neth* **9**, 45 (2015).
  - [8] X. Meng and Z. Guo, *Int. J. Heat Mass Tran.* **100**, 767 (2016).
  - [9] Q. Liu and Y. He, *Physica A: Statistical Mechanics and its Applications* **465**, 742 (2017).
  - [10] F. J. Higuera and J. Jimenez, *Europhysics Letters* **9**, 663 (1989).
  - [11] Y. H. Qian, D. D’Humières, and P. Lallemand, *EPL (Europhysics Letters)* **17**, 479 (1992).
  - [12] H. Chen, S. Chen, and W. H. Matthaeus, *Phys. Rev. A* **45**, R5339 (1992).
  - [13] D. D’Humières, *Rarefied Gas Dynamics- Theory And Simulations*, 450 (1994).
  - [14] X. Y. He and L. S. Luo, *Phys. Rev. E* **56**, 6811 (1997).
  - [15] P. L. Bhatnagar, E. P. Gross, and M. Krook, *Physical review* **94**, 511 (1954).
  - [16] Z. Guo, B. Shi, and C. Zheng, *Int. J. Numer. Meth. Fl.* **39**, 325 (2002).
  - [17] Z. Guo, C. Zheng, and B. Shi, *Phys. Rev. E* **65**, 046308 (2002).
  - [18] X. He, S. Chen, and G. D. Doolen, *J. Comput. Phys.* **146**, 282 (1998).
  - [19] J. Latt, B. Chopard, O. Malaspinas, M. Deville, and A. Michler, *Phys. Rev. E* **77**, 056703 (2008).
  - [20] S. Chen and D. Gary, *Annu. Rev. Fluid Mech.* **30**, 329 (1998).
  - [21] A. A. Mohamad, *Lattice Boltzmann Method: Fundamentals and Engineering Applications with Computer Codes* (Springer, 2011).
  - [22] A. Bardow, I. V. Karlin, and A. A. Gusev, *Europhysics Letters (EPL)* **75**, 434 (2006).
  - [23] S. Chapman and T. G. Cowling, *The mathematical theory of non-uniform gases: an account of the kinetic theory of viscosity, thermal conduction and diffusion in gases* (Cambridge university press, 1970).
  - [24] Y. Hwang, *J. Comput. Phys.* **322**, 52 (2016).
  - [25] Q. Zou and X. He, *Phys. Fluids* **9**, 1591 (1997).
  - [26] T. Inamuro, M. Yoshino, and F. Ogino, *Phys. Fluids* **7**, 2928 (1995).
  - [27] U. Ghia, K. N. Ghia, and C. T. Shin, *J. Comput. Phys.* **48**, 387 (1982).